The Canadian Mineralogist
Vol. 47, pp. 25-38 (2009)
DOI: 10.3749/canmin.47.1.25

PROUDITE: A REDETERMINATION OF ITS CRYSTAL STRUCTURE AND THE PROUDITE–FELBERTALITE HOMOLOGOUS SERIES

WILLIAM G. MUMME

CSIRO Minerals, Box 312, Clayton South, Victoria, 3169, Australia

DAN TOPA

Fachbereich Materialforschung und Physik, Universität Salzburg, Hellbrunnerstrasse 34, A–5020 Salzburg, Austria

EMIL MAKOVICKY[§]

Department of Geography and Geology, University of Copenhagen, Østervoldgade 10, DK–1350 Copenhagen, Denmark

ABSTRACT

The crystal structure of proudite was redetermined with the holotype material from Tennant Creek, Australia, using a Nonius single-crystal diffractometer and Mo$K\alpha$ radiation. Our determination of the structure, based on 3388 observed reflections, yielded an R_1 value of 8.2% for 306 parameters. Proudite is monoclinic, *a* 31.814(1), *b* 4.1002(2), *c* 36.560(1), β 109.266(1)° and space group *C*2/*m*. Results of new electron-microprobe analyses give its composition as $Cu_{1.9}Ag_{0.1}Pb_{15.6}Bi_{20.4}Sb_{0.1}S_{32.4}Se_{14.5}$. We report analytical data for associated phases and for Se-free proudite from Felbertal, Austria, as well. The crystal structure contains 18 large cation sites (Pb, Bi, and mixed positions), a single Cu site, and 24 anion sites, nearly all of them being mixed Se,S sites. It consists of regularly sheared double-layers of octahedra that alternate with stepwise sheared $(100)_{PbS}$ layers, two cation–anion sheets thick. Each straight portion of the former layers is 10 octahedra wide, whereas each straight interval of the PbS-like layers is eight square coordination pyramids (Pb, Bi) wide. Proudite is the highest known member of a homologous series of Pb–Bi–Cu sulfosalts with a mixed character, combining accretion of polyhedra and variable-fit of two layer-type fragments. This series contains proudite, felbertalite, makovickyite and a hypothetical intermediate member not yet known as a pure member, only as a combination with a "makovickyite-like element" in a synthetic selenide. This series is here defined as the proudite–felbertalite homologous series.

Keywords: proudite, crystal structure, proudite–felbertalite homologous series.

SOMMAIRE

Nous avons redéterminé la structure cristalline de la proudite de l'échantillon holotype provenant de Tennant Creek, en Australie, en utilisant un diffractomètre Nonius pour monocristaux et un rayonnement Mo$K\alpha$. Notre détermination de la structure, fondée sur 3388 réflexions observées, a donné une valeur de R_1 de 8.2% pour 306 paramètres. La proudite est monoclinique, *a* 31.814(1), *b* 4.1002(2), *c* 36.560(1), β 109.266(1)°, groupe spatial *C*2/*m*. Les résultats d'analyses obtenues avec une microsonde électronique ont donné la composition $Cu_{1.9}Ag_{0.1}Pb_{15.6}Bi_{20.4}Sb_{0.1}S_{32.4}Se_{14.5}$. Nous décrivons aussi la composition des phases associées et d'un échantillon de proudite dépourvue de Se provenant de Felbertal, en Autriche. La structure contient 18 sites adaptés à de gros cations (Pb, Bi, et positions mixtes), un site unique occupé par le Cu, et 24 sites pour anions, presque entièrement à populations mixtes (Se, S). Elle est faite de couches doubles d'octaèdres cisaillés avec régularité qui alternent avec des couches de $(100)_{PbS}$ cisaillées par paliers, d'une épaisseur de deux feuillets cation–anion. Chaque portion rectiligne de ces couches a une largeur de dix octaèdres, tandis que les intervalles rectilignes des couches de type PbS ont une largeur de huit polyèdres pyramidaux à coordinence carrée contenant (Pb, Bi). La proudite est le membre le plus élevé que l'on connaisse d'une série d'homologues de sulfosels de Pb–Bi–Cu à caractère mixte, fondée sur l'accrétion de polyèdres et l'ajustement dimensionnel de deux fragments en feuillets. La série contient proudite, felbertalite, makovickyite et un membre intermédiaire hypothétique, non encore connu à son état pur, mais seulement en combinaison avec un "élément de type makovickyite" dans un séléniure synthétique. On définit ici cette série, appelée la série d'homologues proudite–felbertalite.

(Traduit par la Rédaction)

Mots-clés: proudite, structure cristalline, série d'homologues proudite–felbertalite.

§ *E-mail address*: emilm@geol.ku.dk

Introduction

Proudite was described by Mumme (1976) as a selenium-bearing sulfosalt, $CuPb_{7.5}Bi_{9.33}(S,Se)_{22}$ from the Juno mine, Tennant Creek, Northern Territory, Australia. The crystal-structure determination then reported indicates a periodically sheared layer structure, consisting of double layers of octahedra that alternate with $(100)_{PbS}$ layers two atomic planes thick. However, details of this structure remained unresolved, especially the configurations in the step areas and at midpoints between them.

The discovery of felbertalite (Topa *et al*. 2000, 2001, Topa 2001), a sheared layer-structure with double layers of octahedra and $(100)_{PbS}$ layers, which has non-sheared intervals shorter than in proudite, and which displays a clearly defined role of Cu in the sheared positions of the structure, made it desirable to re-analyze proudite and to redetermine its crystal structure. A discovery of Se-free proudite in the Felbertal tungsten deposit, Austria (Topa *et al*. 2001), in association with felbertalite, led to a reconsideration of the inevitability of the presence of Se in the structure as well. The current redetermination of the crystal structure of proudite allows us to introduce the concept a new proudite–felbertalite homologous series, in which the accretional and variable layer-fit aspects of homology combine.

Experimental

The sample of proudite studied occurs in form of a massive aggregate of intermeshed tabular crystals with excellent cleavage. Some of them are bent or meet at angular contacts. Flakes of proudite are heavily replaced by a phase that is bright in BSE images, with a composition of selenian cannizzarite ("wittite"), as specified below. In Figure 1a, this topotactic substitution left only disjoined lamellae of proudite. In Figure 1b, selenian cannizzarite is seen to replace proudite along cleavage planes and in a broad zone situated between bent lamellae and an aggregate of randomly oriented tabular crystals. The position of junoite in the mineralization sequence is not clear, although junoite and proudite, and junoite and selenian cannizzarite, show mutual lateral displacements with uncertain relationships in relative age.

Two samples of the original proudite material from the deposit of Tennant Creek, Australia, were analyzed with a JEOL–8600 electron microprobe, controlled by a LINK–*eXL* system, operated at 25 kV, 35 nA, with a beam diameter of 5 μm, and an on-line ZAF–4 correction program. The following natural and synthetic standards and X-ray lines were used: chalcopyrite (Cu*K*α, Fe*K*α), galena (Pb*L*α), stibnite (Sb*L*α), Bi_2S_3 (Bi*L*α, S*K*α), Bi_2Se_3 (Se*K*α), CdTe (Cd*L*α, Te*L*α), and pure metal for Ag*L*α. Analytical results are summarized in Table 1, together with the chemical data on proudite from Tennant Creek and from the new occurrence at the Felbertal tungsten deposit, Austria. There are small but distinct differences compared to the original composition reported by Mumme (1976), with Bi contents higher by more than 1 wt.%. The Tennant Creek material is not quite uniform with respect to the degree of (Ag+Bi)-for-2Pb substitution. Proudite found in discrete crystals from that locality (Fig. 1a) is nearly silver-free, whereas that from the junoite cotype material (sent by

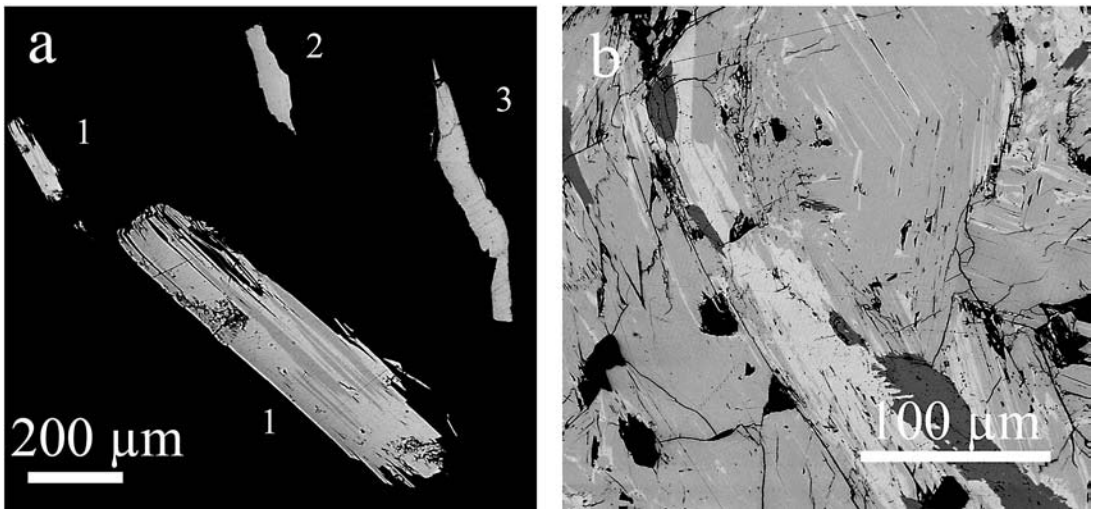

FIG. 1. Back-scattered electron (BSE) photographs of proudite aggregates from Tennant Creek, Australia. Medium grey: proudite, light grey: Se-rich cannizzarite, intense grey: junoite, black: gangue and holes. a) fragment 1 is present both in original size and as an enlarged inset. Scale refers to the general view image.

WGM to Prof. W. Paar, Salzburg, at the time of original description) has distinctly more silver (Table 1). The Felbertal material contains non-negligible amounts of silver and cadmium, with Pb contents still lower, and Bi contents correspondingly higher, than the Tennant Creek material, and with a notable absence of selenium. Compositional fields of cannizzarite, weibullite, proudite, felbertalite and junoite differ sufficiently not to be misinterpreted (Table 2, Fig. 2). In all cases, substitution of Ag + Bi for Pb can visibly modify the position of compositional points in the diagram.

Single-crystal X-ray-diffraction data were collected from the type sample of proudite held in the University of New England collection (R27789), *i.e.*, the same material as was available to Mumme (1976). A Nonius single-crystal diffractometer was used with Mo$K\alpha$ radiation. Data collection and refinement conditions are summarized in Table 3. The unit-cell parameters, *a* 31.814(10), *b* 4.100(10), *c* 36.560 (10) Å, β 109.266(10)°, *V* 4502.0(3) Å^3, differ slightly from the original values obtained by Mumme (1976): *a* 31.96,

TABLE 1. AVERAGE RESULTS OF ELECTRON-MICROPROBE ANALYSES OF PROUDITE FROM TENNANT CREEK AND FELBERTAL

No.	mineral	*n*	Cu	Ag	Pb	Cd	Bi	Sb	Te	Se	S	Total	Ref.
1	proudite	12	1.22(1)	0.15(2)	33.01(12)	-	43.54(20)	0.11(3)	-	11.67(7)	10.60(8)	100.29(19)	1
2	proudite	10	1.23(4)	0.13(2)	33.05(23)	-	43.40(14)	0.11(1)	-	11.78(12)	10.62(8)	100.32(22)	1
3	proudite	11	1.30(2)	0.77(7)	30.67(22)	-	43.85(24)	0.09(2)	-	12.52(16)	10.38(14)	99.57(25)	1
4	FE-98/3-2-gr43-m	6	1.49(4)	1.03(5)	31.36(9)	0.63(6)	48.29(6)	0.15(3)	0.22(5)	-	16.64(9)	99.81(10)	2
5	proudite	-	1.0	-	33.0	-	42.7	-	-	12.8	10.7	100.2	3
6	ideal selenian proudite	-	1.29	-	33.56	-	42.31	-	-	12.79	10.06	100.00	-

Empirical formulae, based on a total of 85 atoms

1) $Cu_{1.89}Ag_{0.13}Pb_{15.61}$ $(Bi_{20.41}Sb_{0.09})_{\Sigma 20.50}$ $(S_{32.39}Se_{14.48})_{\Sigma 46.87}$ or $Cu_{1.89}$ $(Pb+2Ag)_{\Sigma 15.88}$ $(Bi,Ag)_{\Sigma 20.37}$ $(S_{32.39}Se_{14.48})_{\Sigma 46.87}$
2) $Cu_{1.99}Ag_{0.12}Pb_{15.60}$ $(Bi_{20.31}Sb_{0.08})_{\Sigma 20.39}$ $(S_{32.40}Se_{14.60})_{\Sigma 46.99}$ or $Cu_{1.90}$ $(Pb+2Ag)_{\Sigma 15.84}$ $(Bi,Ag)_{\Sigma 20.28}$ $(S_{32.40}Se_{14.60})_{\Sigma 46.99}$
3) $Cu_{2.09}Ag_{0.69}Pb_{14.49}$ $(Bi_{20.53}Sb_{0.08})_{\Sigma 20.61}(S_{31.70}Se_{15.51})_{\Sigma 47.21}$ or $Cu_{2.00}$ $(Pb+2Ag)_{\Sigma 15.87}$ $(Bi,Ag)_{\Sigma 19.92}$ $(S_{31.70}Se_{15.51})_{\Sigma 47.21}$
4) $Cu_{2.11}Ag_{0.86}(Pb_{13.64}Cd_{0.51})_{\Sigma 14.15}$ $(Bi_{20.83}Sb_{0.11})_{\Sigma 20.94}$ $(S_{46.78}Te_{0.15})_{\Sigma 46.93}$ or $Cu_{2.11}$ $(Pb+2Ag)_{\Sigma 15.88}$ $(Bi,Ag)_{\Sigma 20.08}$ $(S_{46.78}Te_{0.15})_{\Sigma 46.93}$
5) $Cu_{1.53}Pb_{15.47}Bi_{19.85}$ $(S_{32.41}Se_{15.75})_{\Sigma 48.16}$
6) $Cu_2Pb_{16}Bi_{20}(S_{31}Se_{16})_{\Sigma 47}$

The compositions are expressed in wt.%. *n*: number of analyses made. The standard deviation for the last digit is shown in brackets. Analysis points: **1** and **2** are two homogeneous grains from Figure 1a (labeled 2 and 3), **3** is the medium grey matrix of Figure 1b (cotype material, Prof. Paar), **4** is the medium grey phase (pr) in the image of Figure 5e of Ref. 2. References: 1) this study, 2) Topa *et al.* (2001), 3) Mumme (1976).

TABLE 2. AVERAGE RESULTS OF ELECTRON-MICROPROBE ANALYSES OF JUNOITE AND PRESUMED Se-RICH CANNIZZARITE FROM TENNANT CREEK

No.	mineral	sample	*n*	Cu	Ag	Pb	Bi	Sb	Se	S	Total	Ref.
1	wittite	Fig. 1a	8	0.06(3)	0.15(2)	34.52(27)	42.46(22)	0.09(4)	12.77(14)	9.85(10)	99.89(47)	1
2	junoite	Fig. 1b	11	3.99(4)	-	19.99(11)	52.43(14)	0.23(7)	10.78(20)	12.18(17)	99.59(26)	1
3	wittite	Fig. 1b	11	0.04(1)	0.52(6)	33.16(21)	42.56(20)	0.07(1)	13.16(13)	9.70(13)	99.23(20)	1
4	weibullite		-	-	1.0	28.3	48.0	-	12.8	10.3	100.4	2
5	wittite		-	-		35.3	43.9		7.7	12.3	99.5	2

Empirical formulae based on total number of atoms *pfu* equal to 35 for junoite, 41 for wittite (Se-rich cannizzarite) and 32 for weibullite

1) $Cu_{1.89}Pb_{3.01}$ $(Bi_{7.84}Sb_{0.06})_{\Sigma 7.90}$ $(S_{11.86}Se_{4.27})_{\Sigma 16.12}$
2) $Cu_{0.02}Ag_{0.24}Pb_{7.82}$ $(Bi_{9.95}Sb_{0.03})_{\Sigma 9.98}$ $(S_{14.79}Se_{8.15})_{\Sigma 22.93}$
3) $Cu_{0.04}Ag_{0.07}Pb_{8.12}$ $(Bi_{9.90}Sb_{0.04})_{\Sigma 9.94}$ $(S_{14.96}Se_{7.88})_{\Sigma 22.84}$
4) $Ag_{0.35}Pb_{5.09}Bi_{8.56}$ $(S_{11.97}Se_{6.04})_{\Sigma 18.01}$
5) $Pb_{6.11}Bi_{9.99}$ $(S_{18.26}Se_{4.64})_{\Sigma 22.90}$

For details, see Table 1. References: 1) this study, 2) Mumme (1980).

b 4.12, ***c*** 36.69 Å, β 109.52°, *V* 4553.5 Å^3. The space group *C*2/*m* is confirmed.

The positions of predominantly Pb,Bi atoms in the unit cell with this space group were located using direct methods (Farrugia 1999). Additional cations (including Cu) and anions were located in successive difference-Fourier maps. Unlike the attempts based upon limited film-based data in 1976, with the benefit of more complete CCD data, a correct solution of the structure with S,Se located at the 2a position in *C*2/*m* was readily achieved in the present case.

The structure was refined to an R_1 value of 0.082 using anion positions with a mixed S,Se occupancy. Anisotropic displacement parameters were used for both the cations and anions. Positional parameters and atomic displacement factors are given in Table 4. A table of structure factors has been deposited in the Depository of Unpublished Data, on the MAC website [document Proudite CM47_25].

Description of the Structure

The crystal structure of proudite contains 18 distinct large-cation sites, a single copper site, and 24 anion sites with a mixed S,Se character. The Pb and Bi sites, or the Pb,Bi mixed sites, could not be distinguished during the structure determination and had to be inferred from the coordination characteristics of their polyhedra.

Our description of the structure is organized following its principal modular features (Fig. 3): alternation of (a) regularly sheared double-layers of octahedra with (b) step-wise sheared $(100)_{PbS}$ layers, two atom sheets thick; the steps in the latter contain tetrahedrally coordinated Cu sites. According to the symmetry of their underlying motifs, these two types of layers have been respectively named pseudohexagonal (H) and pseudotetragonal (Q) slabs, by Makovicky (1989) among others. Each straight portion of the (a) layers is 10 octahedral sites wide, whereas a straight interval of the (b) layers is eight square coordination pyramids wide, with eight crystallographically independent cation sites populating its surfaces. Atom designations are shown in Figure 4.

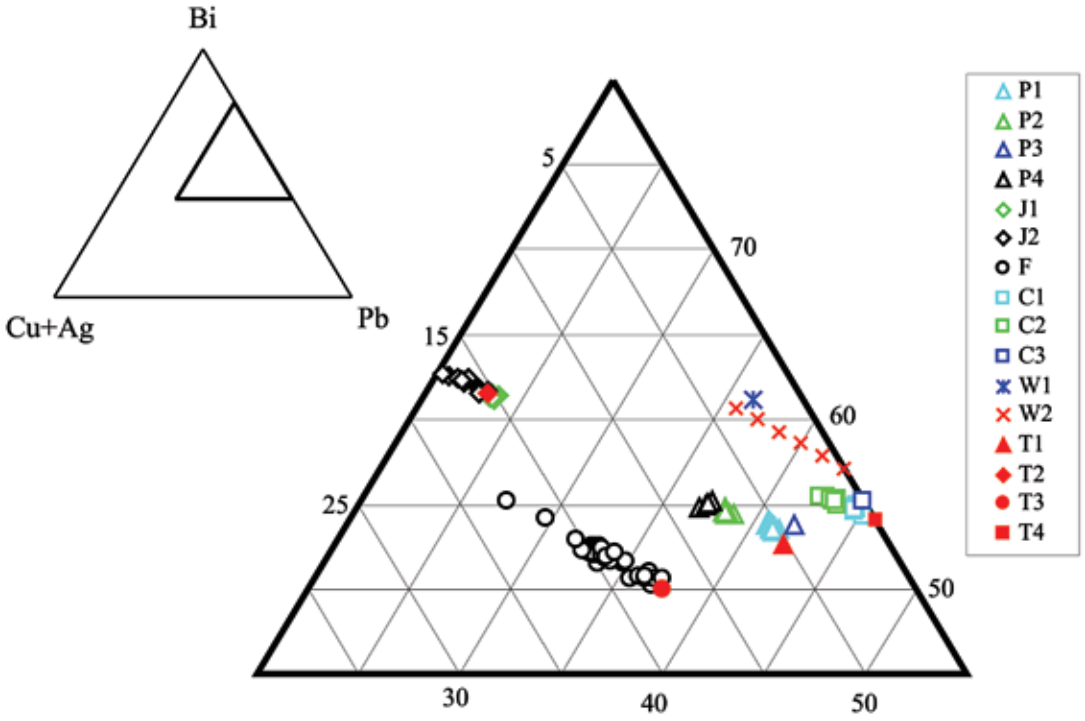

Fig. 2. Compositional data for proudite from Tennant Creek, Australia, and Felbertal, Austria, plotted in the Bi – Pb – (Cu + Ag) composition triangle, together with those of related or associated phases and the ideal compositions derived from structure determination. P: proudite [1–3: Tennant Creek; 1 and 2: analyses from aggregates in Figs. 1a and 1b, respectively; 3: analysis by Mumme (1976); 4: Felbertal]. J: junoite [1: Tennant Creek, 2: Felbertal]. F: Felbertalite [Felbertal]. C: selenian cannizzarrite [1 and 2: Tennant Creek, Figs. 1a and 1b; 3: Mumme (1980)]. W: weibullite [1: Mumme (1980)]. Ideal, structure-derived compositions are indicated in red. The compositional trends observed are due to the (Ag+Bi) for 2Pb substitution.

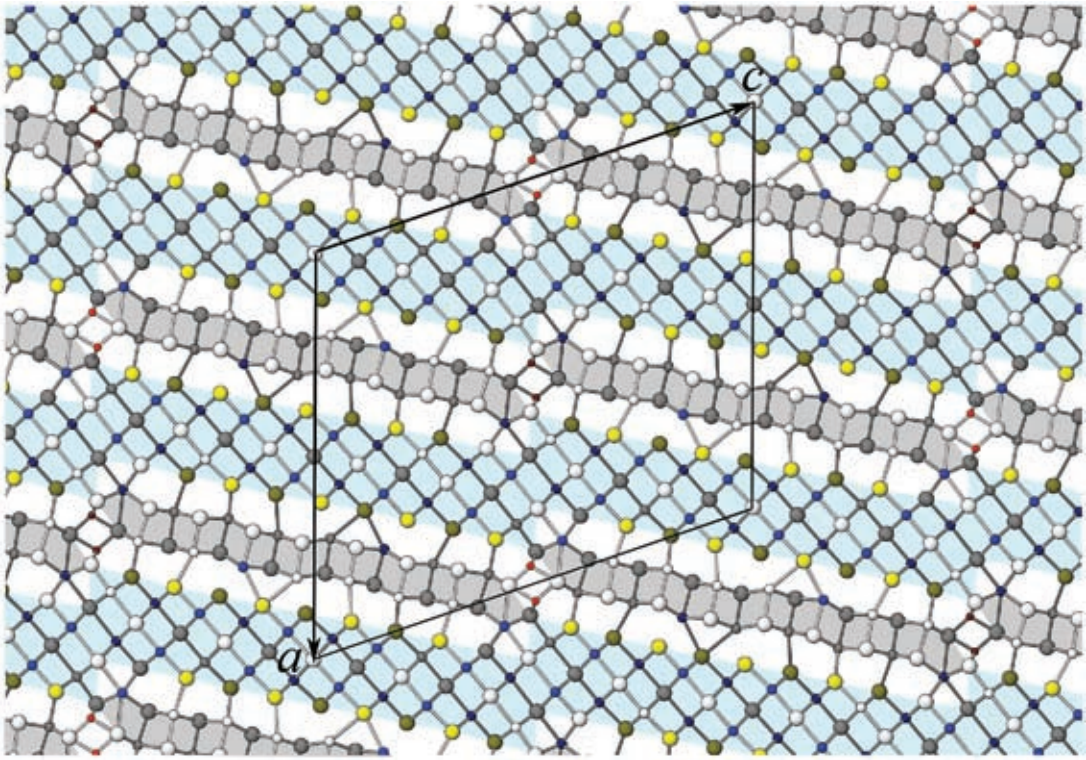

FIG. 3. Modular representation of the crystal structure of proudite. Blue: sheared pseudohexagonal double-octahedron layers, with those positions occupied predominantly by selenium indicated in yellow. Dark grey: pseudotetragonal layer fragments staggered on, and interconnected by, paired Cu tetrahedra (red). Large white spheres: predominantly sulfur sites, small white spheres (predominantly) Bi sites and blue (predominantly) Pb sites. Relative height of atoms, on two (010) planes 2 Å apart, is indicated by shading.

TABLE 3. SUMMARY OF DATA-COLLECTION CONDITIONS AND REFINEMENT PARAMETERS FOR PROUDITE

Crystal data

Chemical formula	$Bi_{29}Cu_2Pb_{16}S_{32.5}Se_{14.5}$	Space group	*C2/m*
a (Å)	31.8143(9)	D_x (Mg m^{-3})	7.288
b (Å)	4.1002(2)	Crystal form	lath
c (Å)	36.560(1)	Crystal size (mm)	0.04 × 0.06
β (°)	109.266(1)		× 0.20
V (Å^3)	4502.0(3)	Crystal color	gray,metallic
Z	2		

Data collection

Collection mode	φ scan, 0-360° Δφ = 0.5° plus ω scan
Temperature (K)	293
Measurement time (s)/frame	40
$2\theta_{max}$ (°)	55.54
Data completeness	96.3%
μ (mm^{-1})	76.37
Absorption correction (SADABS)	T_{min} / T_{max} = 0.69
No. of measured reflections	19189
No. of unique reflections	5876
No. of observed reflections	3388
Criterion for observed reflections	$F > 4\sigma(F)$
R_{int} for observed reflections	0.0762
R_o for observed reflections	0.0790
Range of *h, k, l*	−40 → h → 40, −3 → k → 5, −48 → l → 48

Refinement

Refinement on	F^2
R_1, *wR* (observed reflections)	0.0822, 0.1392
S = *GooF*	0.976
No. of parameter used	306
$\Delta\rho_{max}$ (eÅ^{-3})	8.73; 0.82 Å from Pb2
$\Delta\rho_{min}$ (eÅ^{-3})	−6.35; 0.90 Å from Pb7
Extinction coefficient	none
Source of atomic scattering factors	*International Tables for X-Ray Crystallography* (1992, Vol.C)
Program solution	SHELXS–97 (Sheldrick 1997)

The copper site

The pseudotetragonal (Q) slabs are interrupted in the area of structural steps ($x = 0$, $z = 0.5$) and the two adjacent fragments of them become separated by a column of empty, edge-sharing octahedra. The tetrahedral interspaces between adjacent octahedra of this column repeat periodically along both sides of it, being centered on $x = \pm 0.04$, and are occupied by copper. The Cu–(S,Se) distances range from 2.27 to 2.44 Å, all of them oriented to low-Se positions (Table 5). Two coordination tetrahedra of copper with the same *y* coordinate share an edge, with a Cu–Cu distance equal to 2.75 Å, *i.e.*, a weak cation–cation interaction is present in the structure, typical of copper in chalcogenides.

TABLE 4. POSITIONAL AND ATOMIC DISPLACEMENT PARAMETERS FOR PROUDITE FROM TENNANT CREEK

Atom	sof	*x*	*y*	*z*	U_{eq}	U_{11}	U_{22}	U_{33}	U_{13}
Bi1	1	0.15135(5)	0.5	0.15886(4)	0.0225(4)	0.0319(9)	0.0205(9)	0.0139(6)	0.0059(6)
Pb2	1	-0.14999(5)	0	-0.34867(4)	0.0262(4)	0.0381(9)	0.0221(9)	0.0171(7)	0.0075(6)
Pb3	1	0.09015(5)	0	0.05781(4)	0.0223(4)	0.0341(9)	0.0185(9)	0.0137(7)	0.0071(6)
Pb4	1	0.21068(5)	0	0.25878(4)	0.0251(4)	0.0362(9)	0.0211(9)	0.0166(7)	0.0068(6)
Bi5	1	-0.08572(5)	0.5	-0.24695(4)	0.0274(4)	0.0414(9)	0.0223(9)	0.0178(7)	0.0088(7)
Bi6	1	0.27379(5)	0.5	0.36010(4)	0.0249(4)	0.0365(9)	0.0211(9)	0.0149(7)	0.0054(6)
Pb7	1	-0.02670(5)	0	-0.14503(4)	0.0244(4)	0.0354(9)	0.0213(9)	0.0165(7)	0.0085(6)
Pb8	1	-0.21338(5)	0.5	-0.44900(4)	0.0257(4)	0.0394(9)	0.0206(9)	0.0168(7)	0.0088(6)
Bi9	1	0.33998(5)	0	0.46164(4)	0.0228(4)	0.0318(9)	0.0205(9)	0.0139(7)	0.0048(6)
Pb10	1	0.03458(5)	0.5	-0.04399(4)	0.0252(4)	0.0373(9)	0.0199(9)	0.0164(7)	0.0063(6)
Bi11	1	0.21576(6)	0	0.03788(4)	0.0294(4)	0.0389(9)	0.0269(9)	0.0208(8)	0.0078(7)
Pb12	1	0.28870(6)	0	0.16044(4)	0.0299(4)	0.0442(9)	0.0231(9)	0.0207(8)	0.0080(7)
Bi13	1	0.06023(6)	0.5	-0.39925(4)	0.0339(4)	0.061(1)	0.0216(9)	0.0195(8)	0.0141(7)
Bi14	1	0.16338(5)	0	-0.08141(4)	0.0277(4)	0.040(1)	0.0238(9)	0.0169(7)	0.0062(6)
Bi15	1	0.07985(6)	0	-0.19458(4)	0.0314(4)	0.043(1)	0.0254(9)	0.0253(8)	0.0107(7)
Bi16	1	0.01710(6)	0	-0.31776(4)	0.0298(4)	0.044(1)	0.0253(9)	0.0194(7)	0.0097(7)
Bi17	1	0.36702(6)	0	0.27271(4)	0.0312(4)	0.050(1)	0.0237(9)	0.0178(7)	0.0087(7)
Pb18	1	0.41899(8)	0.5	0.56515(5)	0.0506(6)	0.091(2)	0.035(1)	0.0221(9)	0.0129(9)
Cu1	1	0.0450(2)	0	0.5059(2)	0.052(2)	0.059(4)	0.065(4)	0.033(3)	0.018(3)
(**Se**,S)1	0.85,0.15	0.1197(2)	0.5	0.0175(1)	0.024(2)	0.033(3)	0.021(3)	0.021(2)	0.012(2)
(**Se**,S)2	0.64,0.36	0.1761(2)	0	0.1161(1)	0.018(2)	0.024(3)	0.017(3)	0.011(2)	0.005(2)
(**Se**,S)3	0.81,0.19	0.2363(2)	0.5	0.2137(1)	0.024(2)	0.031(3)	0.022(3)	0.023(2)	0.011(2)
(**Se**,S)4	0.61,0.39	0.2969(2)	0	0.3170(2)	0.027(2)	0.035(3)	0.021(3)	0.025(3)	0.010(2)
(**Se**,S)5	0.78,0.22	0.0600(2)	0	-0.0866(1)	0.028(2)	0.031(3)	0.027(3)	0.026(3)	0.011(2)
(**Se**,S)6	0.72,0.28	-0.0009(2)	0.5	-0.1874(1)	0.030(2)	0.037(3)	0.026(3)	0.028(3)	0.012(2)
(Se,**S**)7	0.44,0.56	-0.0629(2)	0	-0.2884(2)	0.031(2)	0.035(4)	0.027(3)	0.032(4)	0.014(3)
(**Se**,S)8	0.75,0.25	0.3591(2)	0.5	0.4141(1)	0.026(2)	0.036(3)	0.024(3)	0.017(2)	0.007(2)
(Se,**S**)9	0.11,0.89	0.1792(3)	0.5	0.3026(2)	0.021(3)	0.021(5)	0.025(6)	0.014(4)	0.002(3)
(Se,**S**)10	0.04,0.46	0	0	0	0.016(4)	0.019(7)	0.014(7)	0.013(6)	0.003(4)
(**Se**,S)11	0.94,0.06	0.1182(3)	0	0.2016(2)	0.016(3)	0.022(5)	0.016(5)	0.013(4)	0.008(3)
Se12	1	0.0569(3)	0.5	0.1003(2)	0.017(2)	0.018(5)	0.017(5)	0.017(4)	0.007(4)
(Se,**S**)13	0.28,0.72	-0.1272(2)	0.5	-0.3941(2)	0.020(2)	0.034(4)	0.012(4)	0.018(4)	0.015(3)
(Se,**S**)14	0.01,0.99	-0.2416(2)	0	-0.4042(2)	0.017(3)	0.031(6)	0.012(6)	0.007(4)	0.004(4)
(Se,**S**)15	0.12,0.88	0.3194(3)	0.5	0.5095(2)	0.019(3)	0.040(5)	0.012(5)	0.012(4)	0.017(4)
(Se,**S**)16	0.16,0.84	0.1326(3)	0.5	-0.1388(2)	0.029(3)	0.037(5)	0.021(5)	0.024(5)	0.003(4)
(Se,**S**)17	0.14,0.86	0.0539(3)	0.5	-0.2587(2)	0.028(3)	0.039(6)	0.033(6)	0.010(4)	0.005(3)
(Se,**S**)18	0.24,0.76	-0.0123(2)	0.5	-0.3745(2)	0.024(3)	0.030(4)	0.023(5)	0.017(4)	0.003(3)
(Se,**S**)19	0.20,0.80	0.0966(3)	0	-0.3298(2)	0.028(3)	0.040(5)	0.021(5)	0.019(4)	0.005(3)
(Se,**S**)20	0.13,0.87	0.2393(3)	0	-0.0967(2)	0.023(3)	0.033(5)	0.023(5)	0.009(4)	0.003(3)
S21	1	0.1574(3)	0	-0.2130(3)	0.021(2)	0.019(5)	0.019(5)	0.022(5)	0.005(4)
(Se,**S**)22	0.11,0.89	0.2027(3)	0.5	-0.0261(2)	0.030(3)	0.040(6)	0.031(6)	0.020(5)	0.010(4)
(Se,**S**)23	0.05,0.95	0.4236(3)	0	0.5063(2)	0.016(3)	0.020(5)	0.016(5)	0.006(4)	-0.001(3)
(Se,**S**)24	0.08,0.92	-0.0168(3)	0	0.4447(3)	0.031(3)	0.043(7)	0.027(5)	0.023(5)	0.009(4)

sof: site-occupancy factor.

Pseudotetragonal fragments

The $(100)_{PbS}$-based structural fragment contains only low-selenium anion sites (from less than 4 to 14 at.% Se in a site). The marginal Pb18 site is a typical Pb site in a bicapped trigonal prismatic coordination (Table 5, Fig. 4). The opposing, also marginal Bi13 site is a typical square coordination pyramid with an asymmetrical distribution of bonds (Table 5). The interatomic distances are greater than for the corresponding Bi3 position in felbertalite (Topa *et al.* 2000) or in aikinite (Topa 2001), because two of the anion sites involved in the polyhedron have 12–14 at.% Se substituting for S. The Pb12 site is a Pb site, whereas Bi11, in a low-Se environment, and to a lesser degree probably all the other cation sites with the exception of Bi4, are mixed sites with variable proportions of Pb substituting for Bi. All these sites have long cation–anion distances to the heavily Se-substituted anion sites across the non-commensurate interlayer space, which is situated between the pseudotetragonal and pseudohexagonal layers. In this situation, any more exact criteria for distinguishing Pb from Bi (or for assessing the percentages of Pb *versus* Bi in a mixed site), such as polyhedron and circumscribed-sphere volumes (Balić-Žunić & Makovicky 1996) or bond-length hyperbolae (Berlepsch

et al. 2001) cannot be applied without prior corrections for S-for-Se substitution, which are of questionable validity. Performing these, one should choose either a simple subtraction from the bond length observed, based on the comparison of ionic radii for S^{2-} and Se^{2-} and on the percentage of these anions at the site, or a more complex modeling of a change in degree of covalency as a result of this substitution.

Double-octahedron (*pseudohexagonal*) *layers*

The double-octahedron layer contains a set of asymmetric polyhedra surrounding the shear step, and a set of more regular polyhedra forming the fairly monotonous straight portions. A typical asymmetric octahedral (or, where only short distances are considered, square-pyramidal) Bi9 site, with the pyramid apex-to-opposing long-distance ratio equal to 2.62/3.14 Å, shares pyramidal edges with the Pb18 polyhedron from the pseudotetragonal (b) layer and is followed diagonally across the double-octahedron (a) layer by Pb8 and a mixed site "Pb6". The latter site closes the lone-electron-pair micelle developed in the layer-step area of the double-octahedron (a) layer (in which the *M*–S distances are 3.14–3.37 Å) by its short apical bond of 2.78 Å (Figs. 3, 4).

There are no well-expressed lone-electron-pair micelles in the straight portion of the (a) layer of octahedra. The median sheets of anions in it are the purest S positions in the entire structure. The *M*–S distances toward these atoms of sulfur vary over a narrow range 2.96–3.06 Å, whereas those toward the mixed S,Se sites on the layer surface are 2.78–2.92 Å (Table 5). These distances indicate that a shift of all cations toward the layer surface, as well as any potential match problems in the layer interior, are substantially reduced by a selective incorporation of Se into the surface sites.

The cation sites in the straight portions are interpreted as mixed sites; among them, "Pb6" and "Pb1" (Fig. 4) presumably have the largest percentage of Bi within this group of sites, as seen from Table 5.

Modular description: the felbertalite–proudite homologous series

A comparison of the crystal structure of proudite (Fig. 3) with that of *felbertalite* (Topa *et al*. 2000) (Fig. 5, Table 6) shows their wide-ranging similarity: both have double-octahedron layers of a very regular

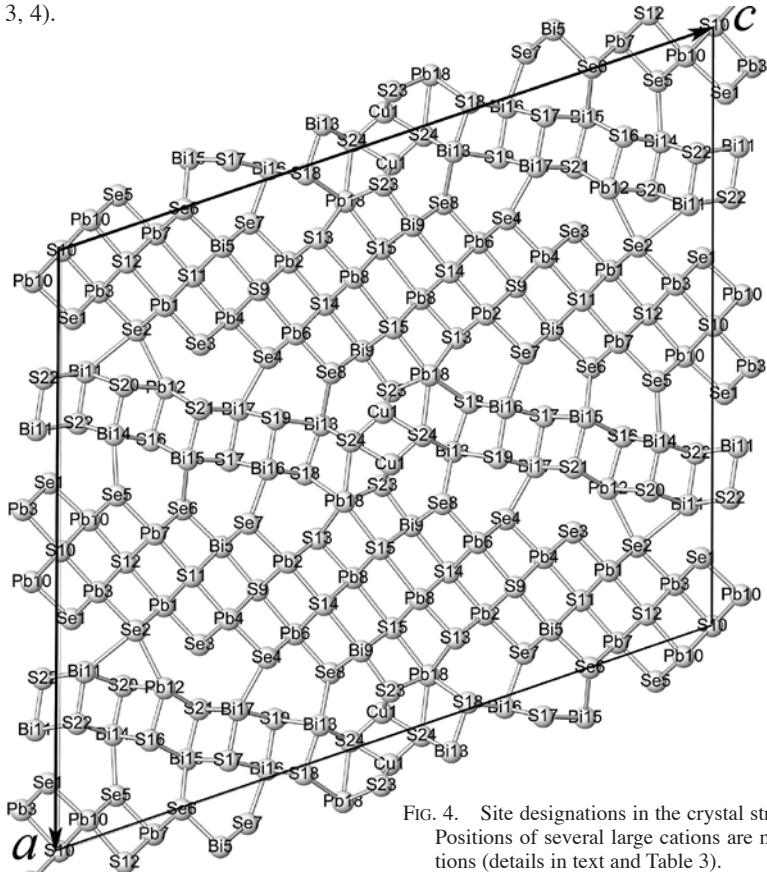

FIG. 4. Site designations in the crystal structure of proudite. Positions of several large cations are mixed (Pb,Bi) positions (details in text and Table 3).

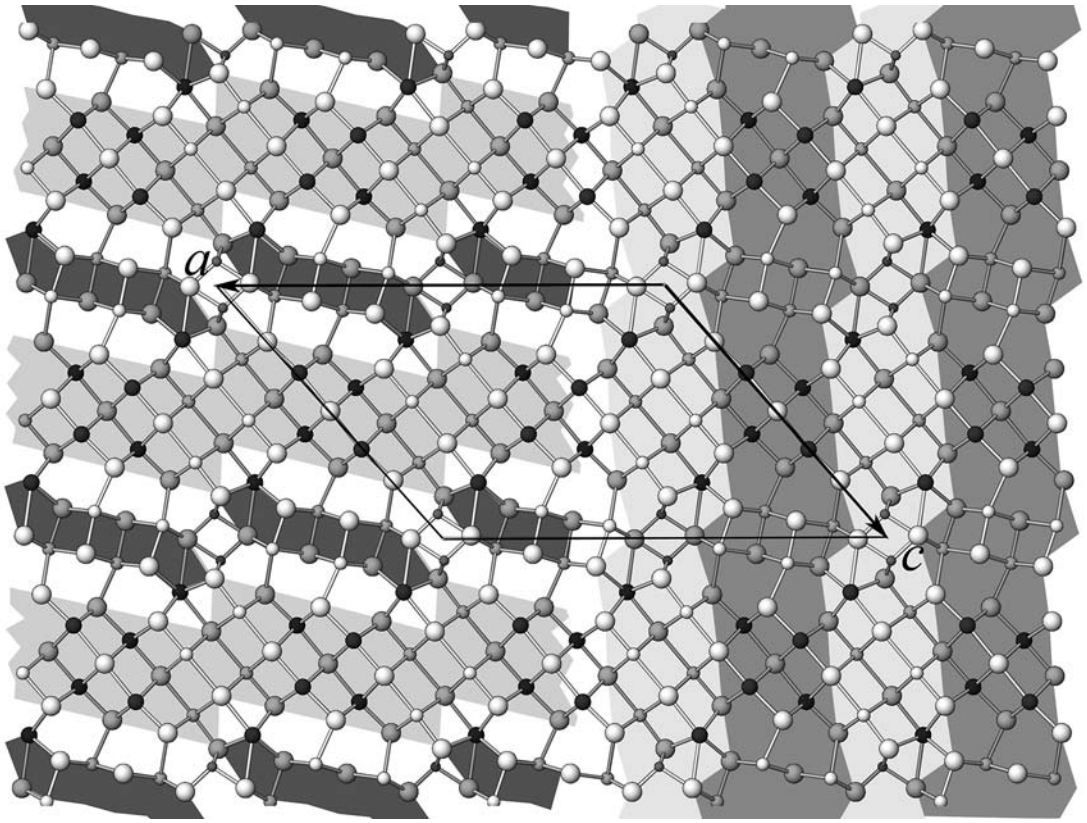

FIG. 5. Modular representation of the crystal structure of felbertalite (Topa *et al*. 2000). Left-hand portion: light grey: sheared double-octahedron layers; dark grey: staggered pseudotetragonal layer fragments; atom designations are analogous to those in Figure 3. Right-hand portion: felberalite as a composite of makovickyite-like slabs (light) interleaved with accretional slabs (medium grey), which convert makovickyite into a higher homologue.

type, with a distinct lone-electron-pair micelle in the step area and cations shifted slightly to the surface, a sheared two-sheet $(100)_{PbS}$ layer with the apical and central polyhedra assuming the same coordinations as in proudite, and a sheared region with a pair of tetrahedral Cu-sites. Moreover, the interlayer match in felbertalite is contained, as an appropriate fragment, in proudite (Fig. 6).

In both structures, the staggered intervals of the (a) layer have no overlap [the shear plane continues across the (a) slab]. The straight hexagonal surface of the (b) layer gives five orthohexagonal, centered subcells (submesh) in a step-to-step interval in proudite, and only two submeshes in felbertalite. In the matching interval of the $(100)_{PbS}$ (a) layer, each square coordination pyramid of Bi(Pb) is a submesh of a pseudotetragonal $(100)_{PbS}$ surface. The surface of a matching fragment of the (a) layer is eight pseudotetragonal subcells wide plus ½ subcell for a half of the octahedron in the column of Cu atoms in proudite and, if it is defined in an analogous way, only 3½ subcells wide in felbertalite.

Thus, felbertalite and proudite are two homologues (Table 6, Fig. 6) in which both the number of polyhedra in two distinct layers and their interlayer match have to be satisfied as the straight interstep intervals become shorter on going from proudite to felbertalite. This type of homologous series was called the *homologous series with a combined character*, combining the accretional and variable-fit characteristics, by Makovicky (1989).

The next lower member of the series are the structures of the *makovickyite – cupromakovickyite* homeotypic pair (Žák *et al*. 1994, Topa & Paar 2008, Topa *et al*. 2008), with the shortest surface of the double-octahedron layer only one orthohexagonal submesh long, and a pseudotetragonal fragment 1½ Q submeshes long (this includes a half of the column of octahedra). The generalized scheme of these structures is shown in Figure 7. Again, the tendency to form slightly inflated

lone-electron-pair micelles is apparent in real structures. The square-pyramidal Bi site belongs clearly to the $(100)_{PbS}$ layer. Columns of octahedra are sites of Cu and Ag positions. However, the foreshortened octahedra of these columns do not allow simultaneous occupancy of the two copper positions, such as was observed in higher homologues and has been illustrated in the schematic Figure 7. Therefore, one of these two copper atoms has to be accommodated in an alternative Cu site in the real structure. Homologous contraction from felbertalite to makovickyite is illustrated in Figure 5.

A member of the series with a fragment width situated between that of proudite and felbertalite (Fig. 8) is unknown so far as a pure structure-type. Slabs of this structure, however, were observed in a synthetic selenide of Cu–Pb–Bi analyzed by Lundegaard *et al.* (in prep.), in which they alternate with thin slabs of makovickyite type. Four orthohexagonal subcells of the double-octahedron pseudohexagonal layer meet with six-and-a-half subcells of the pseudotetragonal layer in this structure. Therefore, mixed types with two regularly alternating lengths of straight fragments can be constructed. The only compound of this type known to us at present is the above-mentioned synthetic selenide. The occasional occurrence of fragments (structure slabs) with the wrong length can be expected, especially in the structures with wide fragments, such as proudite.

A *general formula* for the homologous series with a combined character ties the number of matching subcells with the number of cations and anions *pfu*. There is a difference, however, between these and the formulae derived for pure accretional homologous series (*e.g.,* Makovicky 2006). In the present case, when we use the number of subcells of one of the two components (H or Q) to construct the formula, we must introduce correction terms to take into account the small deviations, observed in real structures, from the model subcell ratios (matches), which we used above for modular description of individual members of the series [these model matches are of the m:(n+½) type in the present case]. Thus, if the number of pseudohexagonal subcells in the matching, straight portions of these structures is denoted as Nh, the formula reads $Cu_2\,M_{7Nh+\Delta M}(S,Se)_{10Nh-1+\Delta S}$, where the correction terms are ΔM = –1, 0, 0 and 1, and ΔS = 0, 0,–2 and –2 for

TABLE 5. BOND DISTANCES IN THE POLYHEDRA IN PROUDITE (Å)

M–S	Distance		*M*–S	Distance	
Bi1 – (**Se**,S)3	2.783(5)		Pb2 – (Se,**S**)13	2.877(6)	× 2
Bi1 – (**Se**,S)2	2.843(5)	× 2	Pb2 – (Se,**S**)7	2.916(7)	
Bi1 – (**Se**,S)11	2.973(7)	× 2	Pb2 – (Se,**S**)14	2.952(9)	
Bi1 – **Se**12	3.062(9)		Pb2 – (Se,**S**)9	2.989(7)	× 2
Pb3 – (**Se**,S)1	2.858(5)	× 2	Pb4 – (**Se**,S)4	2.862(6)	
Pb3 – (**Se**,S)2	2.859(5)		Pb4 – (**Se**,S)3	2.910(5)	× 2
Pb3 – (Se,**S**)10	2.948(2)		Pb4 – (Se,**S**)9	2.972(7)	× 2
Pb3 – **Se**12	2.970(7)	× 2	Pb4 – (**Se**,S)11	2.995(8)	
Bi5 – (Se,**S**)7	2.784(5)	× 2	Bi6 – (**Se**,S)8	2.779(5)	
Bi5 – (**Se**,S)6	2.854(5)		Bi6 – (**Se**,S)4	2.827(5)	× 2
Bi5 – (Se,**S**)9	2.998(8)		Bi6 – (Se,**S**)14	2.990(7)	× 2
Bi5 – (**Se**,S)11	3.026(7)	× 2	Bi6 – (Se,**S**)9	3.050(8)	
Pb7 – (**Se**,S)6	2.848(5)	× 2	Pb8 – (Se,**S**)13	2.813(7)	
Pb7 – (**Se**,S)5	2.879(5)		Pb8 – (Se,**S**)15	2.939(6)	× 2
Pb7 – (**Se**,S)11	2.962(8)		Pb8 – (Se,**S**)14	2.943(7)	× 2
Pb7 – **Se**12	2.972(7)	× 2			
Bi9 – (Se,**S**)23	2.623(8)		Pb10 – (**Se**,S)5	2.848(5)	× 2
Bi9 – (**Se**,S)8	2.879(5)	× 2	Pb10 – (**Se**,S)1	2.894(5)	
Bi9 – (Se,**S**)15	2.906(6)	× 2	Pb10 – **Se**12	2.958(9)	
Bi9 – (Se,**S**)14	3.141(9)		Pb10 – (Se,**S**)10	3.028(4)	× 2
Bi(11) – (Se,**S**)22	2.765(10)		Pb12 – (Se,**S**)16	2.864(9)	
Bi(11) – (Se,**S**)20	2.973(6)	× 2	Pb12 – (Se,**S**)21	2.942(7)	× 2
Bi(11) – (Se,**S**)22	3.034(7)	× 2	Pb12 – **S**20	3.011(6)	× 2
Bi13 – (Se,**S**)24	2.712(7)	× 2	Bi14 – (Se,**S**)20	2.652(9)	
Bi13 – (Se,**S**)18	2.743(8)		Bi14 – (Se,**S**)22	2.862(7)	× 2
Bi13 – (Se,**S**)19	3.171(6)	× 2	Bi14 – (Se,**S**)16	2.866(7)	× 2
			Bi14 – (**Se**,S)5	3.231(5)	
Bi15 – **S**21	2.764(10)		Bi16 – (Se,**S**)19	2.706(9)	
Bi15 – (Se,**S**)16	2.986(7)	× 2	Bi16 – (Se,**S**)18	2.847(6)	× 2
Bi15 – (Se,**S**)17	3.018(6)	× 2	Bi16 – (Se,**S**)17	2.926(6)	× 2
			Bi16 – (Se,**S**)7	3.072(7)	
Bi17 – (Se,**S**)17	2.728(9)		Pb18 – (Se,**S**)23	3.010(7)	× 2
Bi17 – (Se,**S**)19	2.881(6)	× 2	Pb18 – (Se,**S**)15	3.151(9)	
Bi17 – **S**21	2.908(7)	× 2	Pb18 – (Se,**S**)13	3.168(6)	× 2
Bi17 – (**Se**,S)4	3.160(6)		Pb18 – (Se,**S**)24	3.248(11)	
			Pb18 – (Se,**S**)18	3.265(6)	× 2
Cu1 – (Se,**S**)24	2.267(11)		Cu1-Cu1	2.751(13)	
Cu1 – (Se,**S**)23	2.386(7)	× 2			
Cu1 – (Se,**S**)24	2.443(11)				

TABLE 6. MEMBERS OF THE PROUDITE – FELBERTALITE HOMOLOGOUS SERIES AND A RELATED PHASE

Mineral	Formula	Lattice parameters				Z	Space group	Q	H	Ref.
		a	*b*	*c*	β					
Proudite	$Cu_2Pb_{16}Bi_{20}(S,Se)_{47}$	31.81	4.10	36.56	109.27	2	*C*2/*m*	8½	5	1
Hypothetical	$Cu_2M_{28}S_{37}$	31.70	4.00	32.00	119.00	4	*C*2/*m*	6½	4	1
Felbertalite	$Cu_2Pb_6Bi_8S_{19}$	27.64	4.05	20.74	131.26	2	*C*2/*m*	3½	2	2
Makovickyite	$Cu_{1.1}Ag_{0.8}Pb_{0.2}Bi_{5.3}S_9$	13.24	4.06	14.67	99.4	2	*C*2/*m*	1½	1	3
Synthetic	$K_{0.7}Sn_{4.8}Bi_{11.2}Se_{22}$	15.78	4.17	17.36	99.25	1	*P*2/*m*	3 + ¾ K*	2½	4
Junoite	$Cu_2Pb_3Bi_8(S,Se)_{16}$	26.66	4.06	17.03	127.20	2	*C*2/*m*	3½	2	5

Q and H refer to the number of respective subcells in the Q:H match. K* denotes a coordination polyhedron of potassium. References: 1) this study, 2) Topa *et al.* (2000), 3) Topa *et al.* (2008), 4) Mrotzek *et al.* (2000), 5) Mumme (1975).

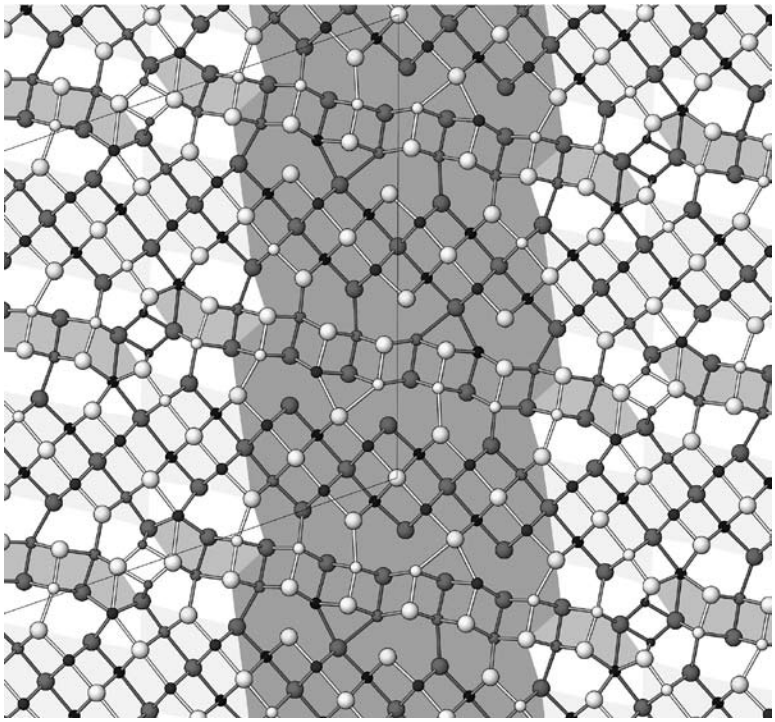

FIG. 6. An interval of the crystal structure of proudite as a composite of the felbertalite-like part (step areas, uncolored) and a large accretional block (solid color), which converts felbertalite into proudite.

the phases that contain 1, 2, 4, and 5 pseudohexagonal subcells matching with 1½, 3½, 6½, and 8½ pseudotetragonal subcells, respectively.

Further relationships

The felbertalite – proudite homologous series with combined character is not isolated: its lowermost member, makovickyite, also belongs to another series, the *pavonite homologous series* of accretional type, whereas felbertalite has *accretional homologues* in junoite and (partly) neyite. This does not invalidate the felbertalite–proudite series: the intersection of two different homologous series in a common member whose crystal structure allows homologous expansion in two different ways is observed both among sulfosalts and silicates (Ferraris *et al*. 2004).

Felbertalite and junoite also are particular cases of so-called "*sliding series*" in which the mutual position of indentations ("steps") on the opposing sides of the (double or single, respectively, in the two compounds) layer of octahedra varies [references in Ferraris *et al*. (2004) and Makovicky (2006)]. One of the hypothetical sliding variants of felbertalite is illustrated in Figure 9. It should be noted that a structure with double-octahedron layers with a given "sliding overlap" of adjacent portions, such as in Figures 5 and 9, can also be described as a structure composed of single-octahedron layers, with another, more extensive overlap (Makovicky 1981).

All structures of this series have *cannizzarite* as a parent structure, in which the step-like shear seen in our structures "occurs at infinitely long intervals", *i.e*., it is absent. The non-sheared intervals of all members of the series are found as intervals in cannizzarite. As Figure 10 reveals, these portions invariably comprise a fragment of the *pseudotetragonal* layer and a fragment of one or both adjacent pseudohexagonal layers of cannizzarite, together with their interlayer match. Match patterns on the two opposing sides of an individual *pseudohexagonal* layer in proudite–felbertalite homologues are in every case mutually displaced if compared to those in cannizzarite. Therefore, these homologues cannot be interpreted as simple intergrowths of shear areas and slabs of cannizzarite of different widths.

A structure closely related to the felbertalite – proudite series is that of $K_{0.66}Sn_{4.82}Bi_{11.18}Se_{22}$ (Mrotzek *et al*. 2000) (Fig. 11). Here, the straight portions of

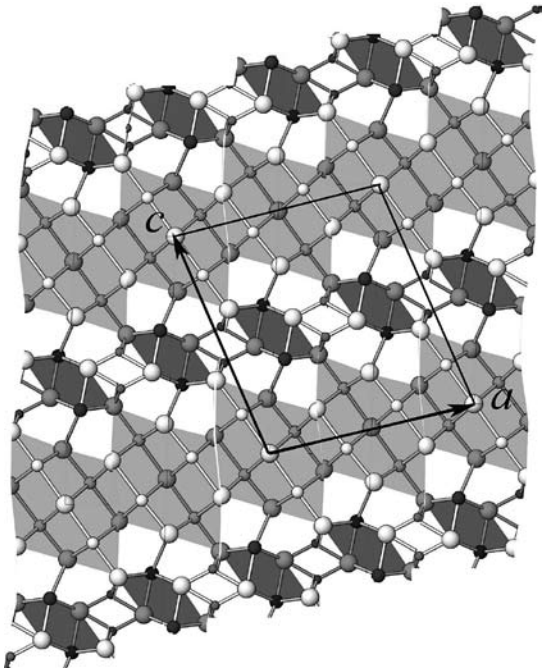

the double-octahedron layer are 2½ pseudohexagonal submeshes long, and those of the pseudotetragonal $(100)_{PbS}$ layer, only 3 pseudotetragonal subcells long. The difference resides in the presence of a hexagonal channel housing a large cation K in place of the column of octahedra that houses copper, as was seen in proudite. As a consequence, the adjacent double-octahedron layers are shifted by a width of one octahedron *versus* the simple situation in which shear planes are continuous across the stacks of layers, as seen in proudite. The Sn site in the structure of this synthetic K–Sn–Bi selenide approximates the marginal Pb in proudite, and other details of this structure are similar to proudite and felbertalite as well.

FIG. 7. A schematic representation of modular principles for the crystal structure of cupromakovickyite (Topa *et al.* 2008). Slab and atom designations as in Figure 5.

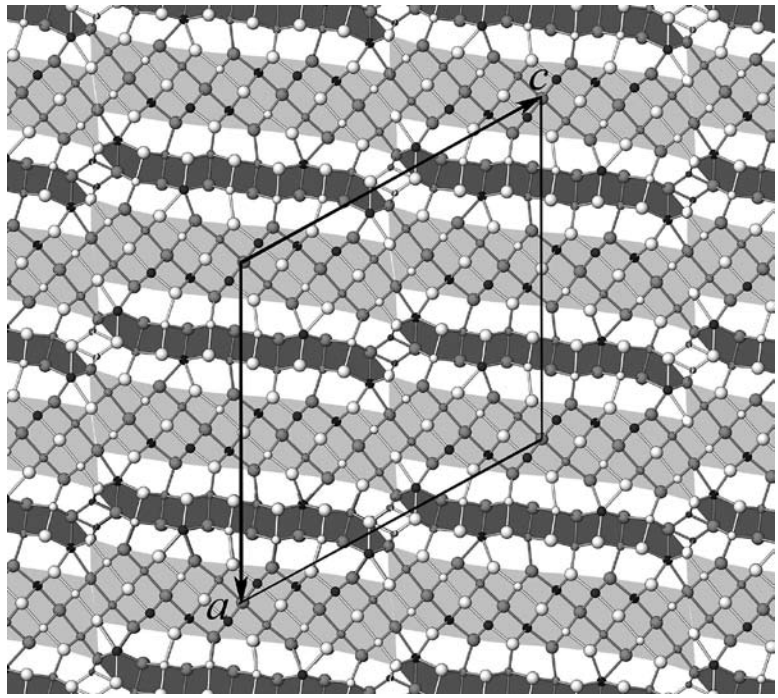

FIG. 8. A hypothetical homologue of proudite based on the width of layer fragments observed in the structure of a synthetic Cu–Pb–Bi selenide with two alternating intervals of different width (Lundegaard *et al.*, in prep.). It is a member situated between proudite and felbertalite.

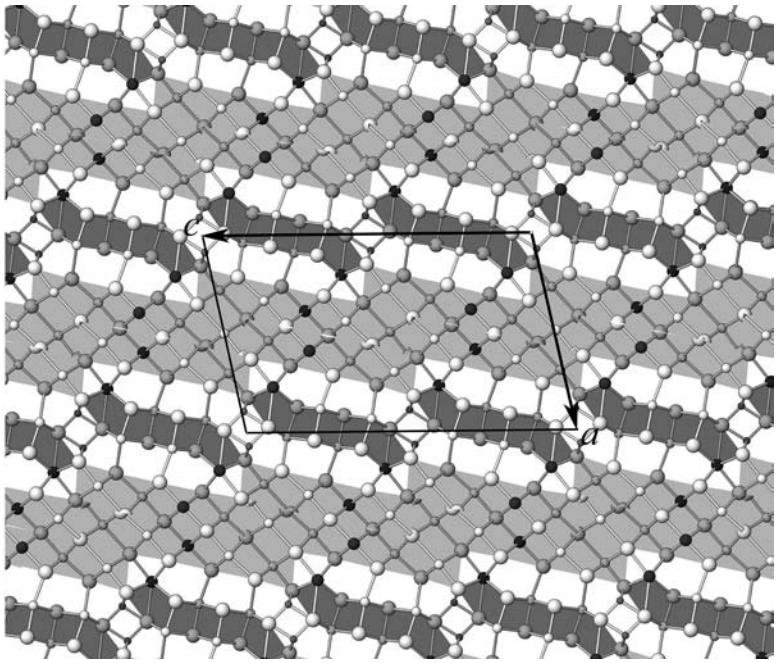

FIG. 9. A sliding variant of the felbertalite structure, with shear indentations on the opposing sides of the double-octahedron layer displaced by a width of one octahedron *versus* the original situation. The ideal composition is $Cu_2M_{15}S_{20}$.

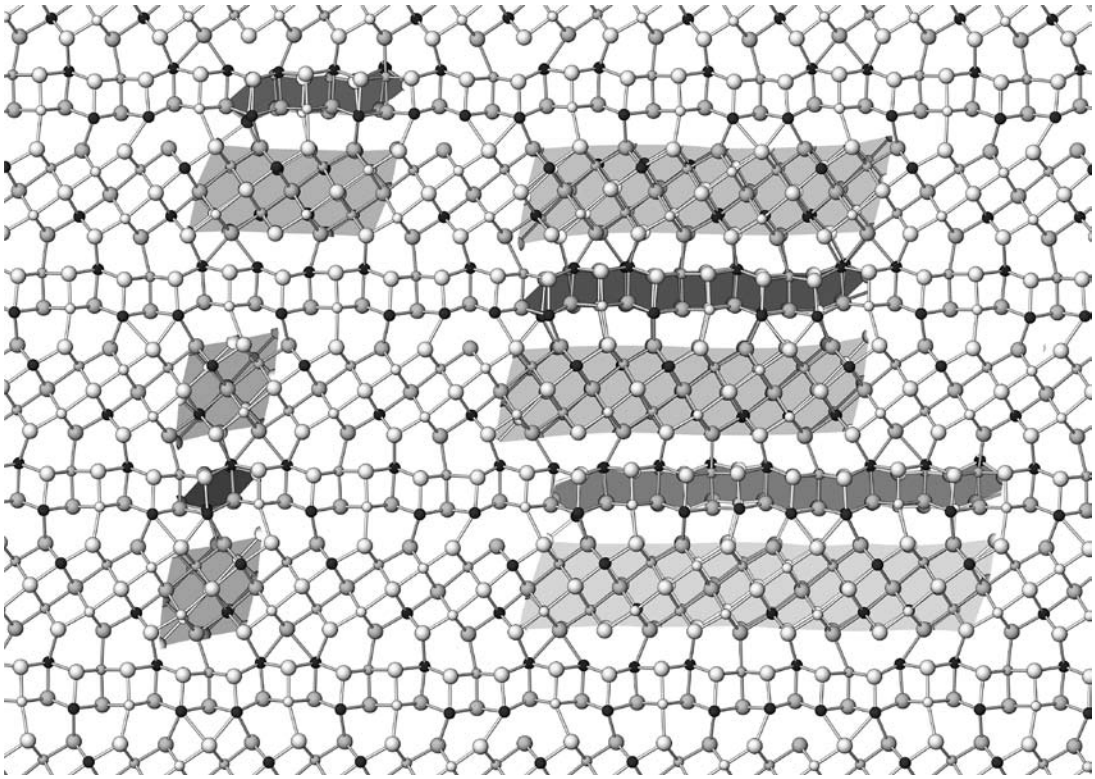

FIG. 10. Crystal structure of cannizzarite (Matzat 1979) with intervals superimposed by, in the order of increasing length, the straight layer portions of makovickyite, of felbertalite, of a hypothetical homologue from Figure 8, and of proudite, respectively, pasted in. Pseudotetragonal layers: dark grey, pseudohexagonal layers: light grey. Large spheres: anions, small spheres: cations.

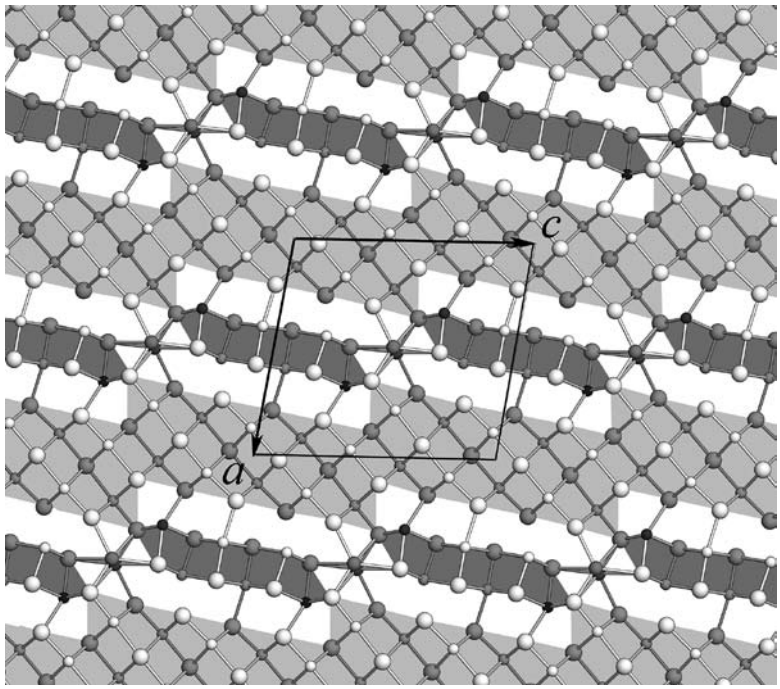

FIG. 11. The crystal structure of $K_{0.66}Sn_{4.82}Bi_{11.18}Se_{22}$ (Mrotzek *et al*. 2000). Se: large spheres, Sn: black, Bi: small spheres, K: grey in unshaded [001] channels.

ACKNOWLEDGEMENTS

We thank to Dr. Garry Fallon of the Department of Chemistry, Monash University, for his kind assistance with the experimental work. Support by the project no. 21–03–0519 of the National Research Council for Natural Science (Denmark) and by the Christian Doppler Research Society (Austria) is gratefully acknowledged. Valuable comments of two anonymous referees and the editorial care of Prof. Robert F. Martin are highly appreciated.

REFERENCES

BALIĆ-ŽUNIĆ, T. & MAKOVICKY, E. (1996): Determination of the centroid or 'the best centre' of a coordination polyhedron. *Acta Crystallogr.* **B52**, 78-81.

BERLEPSCH, P., MAKOVICKY, E. & BALIĆ-ŽUNIĆ, T. (2001): Crystal chemistry of meneghinite homologues and related sulfosalts. *Neues Jahrb. Mineral., Monatsh.*, 115-135.

FARRUGIA, L.J. (1999): WINGX suite for small-molecule single-crystal crystallography. *J. Appl. Crystallogr.* **32**, 837-838.

FERRARIS, G., MAKOVICKY, E. & MERLINO, S. (2004): *Crystallography of Modular Materials*. Oxford University Press, Oxford, U.K.

MAKOVICKY, E. (1981): The building principles and classification of bismuth–lead sulfosalts and related compounds. *Fortschr. Mineral.* **59**, 137-190.

MAKOVICKY, E. (1989): Modular classification of sulfosalts – current status: definition and application of homologous series. *Neues Jahrb. Mineral., Abh.* **160**, 269-297.

MAKOVICKY, E. (2006): Crystal structures of sulfides and other chalcogenides. *In* Sulfide Mineralogy and Geochemistry (D.J. Vaughan, ed.). *Rev. Mineral. Geochem.* **61**, 7-125.

MATZAT, E. (1979): Cannizzarite. *Acta Crystallogr.* **B35**, 133-136.

MROTZEK, A., CHUNG, DUCK-YOUNG, HOGAN, T. & KANATZIDIS, M.G. (2000): Structure and thermoelectric properties of the new quaternary tin selenide $K_{1-x}Sn_{5-x}Bi_{11+x}Se_{22}$. *J. Mater. Chem.* **10**, 1667-1672.

MUMME, W.G. (1975): Junoite, $Cu_2Pb_3Bi_8(S, Se)_{16}$, a new sulfosalt from Tennant Creek, Australia: its crystal-structure and relationship with other bismuth sulfosalts. *Am. Mineral.* **60**, 548-558.

MUMME, W.G. (1976): Proudite from Tennant Creek, Northern Territory, Australia: its crystal structure and relationship to weibullite and wittite. *Am. Mineral.* **61**, 839-852.

MUMME, W.G. (1980): Seleniferous lead–bismuth sulphosalts from Falun, Sweden: weibullite, wittite, and nordströmite. *Am. Mineral.* **65**, 789-796.

SHELDRICK, G.M. (1997): SHELXL-97, *a Program for Crystal Structure Refinement*. University of Göttingen, Göttingen, Germany.

TOPA, D. (2001): *Mineralogy, Crystal Structure and Crystal Chemistry of the Bismuthinite–Aikinite Series from Felbertal, Austria*. Ph.D. thesis, Univ. of Salzburg, Salzburg, Austria.

TOPA, D., MAKOVICKY, E., BALIĆ-ŽUNIĆ, T. (2008): What is the reason for the doubled unit-cell volumes of copper–lead-rich pavonite homologues? The crystal structures of cupromakovickyite and makovickyite. *Can. Mineral.* **46**, 515-523.

TOPA, D., MAKOVICKY, E., BALIĆ-ŽUNIĆ, T. & BERLEPSCH, P. (2000): The crystal structure of $Cu_2Pb_6Bi_8S_{19}$. *Eur. J. Mineral.* **12**, 825-833.

TOPA, D., MAKOVICKY, E., CRIDDLE, A.J., PAAR, W.H. & BALIĆ-ŽUNIĆ, T. (2001): Felbertalite, $Cu_2Pb_6Bi_8S_{19}$, a new mineral from Felbertal, Salzburg Province, Austria. *Eur. J. Mineral.* **13**, 961-972.

TOPA, D. & PAAR, W.H. (2008): Cupromakovickyite, $Cu_8Pb_4Ag_2Bi_{18}S_{36}$, a new mineral species of the pavonite homologous series. *Can. Mineral.* **46**, 503-514.

ŽÁK, L., FRYDA, J., MUMME, W.G. & PAAR, W.H. (1994): Makovickyite, $Ag_{1.5}Bi_{5.5}S_9$ from Băiţa Bihorului, Romania. The ^{4}P natural member of the pavonite series. *Neues Jahrb. Mineral., Abh.,* **168**, 147-169.

Received December 12, 2007, revised manuscript accepted December 13, 2008.